

## TRANSIENT ADJOINT SENSITIVITIES FOR DISCONTINUITIES WITH GAUSSIAN MATERIAL DISTRIBUTIONS

**A. G. Radwan**

Department of Applied Physics and Mathematics  
Faculty of Engineering  
Cairo University, Egypt

**M. H. Bakr and N. K. Nikolova**

Department of Electrical and Computer Engineering  
McMaster University, Hamilton, ON L8S 4K1, Canada

**Abstract**—We present a novel approach for adjoint transient sensitivity analysis with respect to discontinuities with space-dependent materials exhibiting known distribution. Our approach integrates the Time Domain Transmission-Line-Modeling (TD-TLM) with the Adjoint Variable Method (AVM). Using only one extra TD-TLM simulation, the sensitivities of the observed response with respect to all the parameters of the Gaussian distribution are obtained. The accuracy of our sensitivity analysis approach is illustrated through a number of different 2D and 3D examples. Using the previous sensitivities, gradient-based optimization technique is applied to exploit in the location and profile of various inhomogeneous material Gaussian distribution for inverse problems. This method can be repeated for any continuous or discontinuous distributions that exist in electromagnetic imaging for space dependent materials like cancer detection.

### 1. INTRODUCTION

The sensitivity analysis of large-scale systems governed by both ordinary differential equations (ODEs) and partial differential equations (PDEs) has been the subject of extensive research [1–4]. The sensitivity analysis generates information essential in different

applications such as model development, optimization, parameter estimation, model simplification, optimal control, uncertainty analysis, and experimental design [5]. Forward sensitivities can be computed reliably and efficiently via automatic differentiation. However, the forward sensitivity approach is intractable in systems having large number of parameters [3]. It is thus preferable to use adjoint sensitivity algorithms that efficiently calculate the derivatives of an objective function with respect to all parameters using at most one extra simulation.

The applications of adjoint sensitivity analysis have been discussed in many areas [6, 7]. Recently, the use of AVM has been extended to sensitivity analysis with numerical electromagnetic techniques [8–11]. Using only one extra electromagnetic (EM) simulation, the sensitivities of the desired response can be estimated with respect to all parameters. Novel adjoint-based sensitivity analysis algorithms were introduced [12–17]. These algorithms efficiently estimate the objective function sensitivities for different EM structures with different time domain techniques. In [18], it was shown that the sensitivity of any field components  $E(t)$  can be estimated with respect to all the desirable parameters using only one EM simulation regardless of the number of parameters for all time steps.

The adjoint technique is used as a tool for efficiently determining the optimal solutions in different domains [19–21]. One of the main applications of AVM method is the efficient solution of inverse problems. These problems aim at determining the location and material properties of different discontinuities using the EM responses and their available sensitivities.

An important inverse problem is the detection of host medium within the human body [22–24]. However, all these techniques assume that the profile of the host-medium is constant versus space to reduce the optimization variables, or solving for the permittivity and conductivity at each voxel in the computational domain. This large number of optimization variables may also cause non unique solutions.

In this paper, the technique proposed in [18] is extended for space-dependent permittivity and conductivity. We assume a Gaussian distribution for both the relative permittivity and the conductivity. We show that the sensitivities of any desired response with respect to the parameters of these Gaussian distributions are obtained using only one extra adjoint simulation. Also, we demonstrate that this approach is applicable for different excitation sources, different discontinuities, and different observation points. Our approach also limits the optimizable parameters to only the parameters of the Gaussian distribution. This paper is organized as follows; In Section 2, we briefly review the basics

of the Gaussian distribution, the TLM method, and the AVM with the TLM method. Our algorithm is introduced in Section 3. The application of our technique to sensitivity analysis of several structures is illustrated in Section 4. In Section 5, our sensitivity analysis estimates are utilized in the solution of a number of inverse scattering problems. Then, conclusion is given in the last section.

## 2. GENERAL BACKGROUND

### 2.1. The Gaussian Distribution

Different fields of science utilize the Gaussian distribution to approximate non uniform distributions. Here, we assume that the considered discontinuities have relative permittivity  $\varepsilon_r$  and conductivity  $\sigma$  varying according to such a distribution. For 2D and 3D EM problems, the distribution of the relative permittivity, for example, is given by:

$$\begin{aligned}\varepsilon_r(x, z) &= \varepsilon_{r,m} + (\varepsilon_{r,\max} - \varepsilon_{r,m}) \\ &\quad \exp\left(-\left(a(x-x_c)^2 + 2b(x-x_c)(z-z_c) + c(z-z_c)^2\right)\right) \quad (1) \\ \varepsilon_r(x, y, z) &= \varepsilon_{r,m} + (\varepsilon_{r,\max} - \varepsilon_{r,m}) \\ &\quad \exp\left(-\left(\frac{(x-x_c)^2}{2\sigma_x^2} + \frac{(y-y_c)^2}{2\sigma_y^2} + \frac{(z-z_c)^2}{2\sigma_z^2}\right)\right) \quad (2)\end{aligned}$$

where  $(x_c, y_c, z_c)$  is the distribution central point.  $\varepsilon_{r,m}$  and  $\varepsilon_{r,\max}$  are the relative permittivity of the background medium and the maximum value of the relative permittivity at the center, respectively. The parameters  $(\sigma_x, \sigma_y, \sigma_z)$  are the standard deviations along the  $x$ ,  $y$ , and  $z$  directions, respectively. The parameters  $a$ ,  $b$  and  $c$  in (1) are related to the angle of rotation  $\theta$  and the standard deviations as follows:

$$\begin{aligned}a &= \frac{\cos^2(\theta)}{2\sigma_x^2} + \frac{\sin^2(\theta)}{2\sigma_z^2}, & b &= -\frac{\sin(2\theta)}{4\sigma_x^2} + \frac{\sin(2\theta)}{4\sigma_z^2}, \\ c &= \frac{\sin^2(\theta)}{2\sigma_x^2} + \frac{\cos^2(\theta)}{2\sigma_z^2}\end{aligned} \quad (3)$$

If the standard deviations are equal, i.e.,  $\sigma_x = \sigma_y = \sigma_z = \sigma_r$  then (1) will be independent of  $\theta$ . In this case,  $a = c = 1/(2\sigma_r^2)$ , and  $b = 0$ . This distribution is referred to as a polar Gaussian distribution. Expressions similar to (1) and (2) can be written for the conductivity where  $\sigma_m$  and  $\sigma_{\max}$  denote the conductivity of the host medium and the maximum value of the conductivity at the distribution center, respectively. From the different Gaussian functions, we see that the number of parameters of the distribution is six for the 2D case and seven for the 3D case. The

number of unknown parameters in an inverse modeling problem with a Gaussian discontinuity is thus fixed regardless of the number of cells in the computational domain.

## 2.2. Transmission-line-modeling (TLM)

In the TLM method, the medium is modeled by a network of transmission lines where voltages and currents model electric and magnetic fields. Fig. 1 shows the 2D-TLM shunt-node model and the 3D Symmetrical-Condensed-Node (SCN) [26]. The propagation of the electromagnetic fields is simulated by the propagation and scattering of voltage impulses. Every node receives incident voltage impulses that scatter at the center of the node at each time step. The basic iteration for a TLM problem with nondispersive boundaries is given by [27]:

$$\mathbf{V}_{(k+1)} = \mathbf{C}\mathbf{S}\mathbf{V}_k + \mathbf{V}_k^s \quad (4)$$

where  $\mathbf{V}_k$  is the vector of incident impulses for all links at the  $k$ th time step. The matrix  $\mathbf{S}$  is a block diagonal matrix whose  $j$ th diagonal block is the scattering matrix  $\mathbf{S}_j$  of the  $j$ th node. The matrix  $\mathbf{C}$  is the connection matrix of the whole domain and the term  $\mathbf{V}_k^s$  represents the excitation vector at the  $k$ th time step.

## 2.3. Adjoint Variable Method (AVM)

The calculation of the response gradient using finite difference techniques requires at least  $N$  extra EM simulations, where  $N$  is the number of parameters. If  $N$  is relatively large or the simulation is time-intensive, the finite difference techniques become inefficient. The

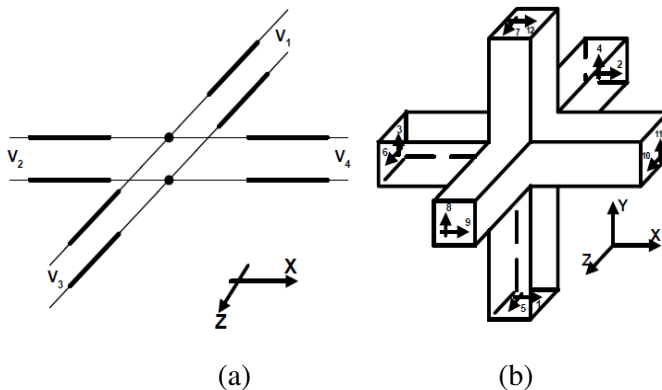


**Figure 1.** The TLM nodes for: (a) the 2D case, and (b) the 3D case.

theory of the Adjoint Variable Method (AVM) sensitivity analysis offers an efficient alternative. Using at most one extra simulation, the sensitivities of the objective function with respect to all parameters can be efficiently estimated regardless of the number of parameters. Several AVM techniques have been developed for sensitivity analysis with different numerical approaches [8–21]. These include the Finite-Element-Time-Domain (FETD) [8], Finite-Element-Frequency-Domain (FEFD) [9], Method of Moments (MoM) [20, 21], Finite-Difference-Time-Domain (FDTD) [15], Frequency Domain TLM (FD-TLM) [11], and TD-TLM [13, 14, 18]. It was assumed in all these techniques that the material properties are constants within the discontinuity of interest.

#### 2.4. AVM for Transient Analysis Using the TLM Technique

The application of the AVM method for sensitivity analysis of time domain responses was presented in [18]. This approach estimates the sensitivity of the temporal electric field calculated at the observation point with respect to a parameter  $p_i$  at time  $\tau$  using the expression:

$$\frac{\partial E(\tau)}{\partial p_i} \approx -\Delta t \sum_k \sum_j \boldsymbol{\lambda}_{j,k,\tau}^T \boldsymbol{\eta}_{j,k,i}, \quad \boldsymbol{\eta}_{j,k,i} = \mathbf{C} \frac{\Delta \mathbf{S}_j}{\Delta p_i} \mathbf{V}_{j,k} \quad (5)$$

where  $\boldsymbol{\eta}_{j,k,i}$  is a vector estimated through the original simulation.  $E(t)$  is any field component,  $p_i$  is the  $i$ th parameter,  $k$  is the time index, and  $j$  is the index of cells affected by a change in  $p_i$ . The vector  $\boldsymbol{\lambda}_{j,k,\tau}$  is the adjoint response of the  $j$ th node at the  $k$ th time step [13]. The vector  $\boldsymbol{\lambda}_{j,k,\tau}$ , for each  $\tau$ , is a shifted version of the adjoint response  $\boldsymbol{\lambda}$  obtained through the adjoint simulation [18]:

$$\boldsymbol{\lambda}_{k-1} \equiv \mathbf{S}^T \mathbf{C} \boldsymbol{\lambda}_k - \Delta t \frac{\partial E(k\Delta t)}{\partial \mathbf{V}} \boldsymbol{\delta}(k\Delta t - T_m), \quad \boldsymbol{\lambda}(T_m) = 0 \quad (6)$$

where  $T_m$  is the simulation time. From (5), it is obvious that  $\boldsymbol{\eta}_{j,k,i}$  depends on the sensitivity of the local scattering matrix with respect to the parameter  $p_i$ .

### 3. AVM FOR GAUSSIAN DISTRIBUTIONS

In this section, we show how the theory presented in [18] is extended to sensitivity analysis with respect to discontinuities exhibiting a Gaussian distribution.

### 3.1. Our AVM Approach

The sensitivity analysis discussed in [18] addresses the case of a single source, a single discontinuity, and a single observation point. It also assumes that the material properties are uniform within the discontinuity. This sensitivity analysis approach requires two simulations, the forward simulation to calculate  $\boldsymbol{\eta}_{j,k,i}$  and the adjoint simulation to calculate  $\boldsymbol{\lambda}_{j,k,\tau}$ . Since the adjoint excitation in this case is independent of the incident voltages  $\mathbf{V}_k$  at any observation point, the forward and the adjoint systems are independent. We can thus carry out both simulations in parallel. We generalize this solution to apply for any number of excitation points, multiple obstacles, and multiple observation points. We assume that the properties of the objects inside the computational domain can be expressed as a Gaussian distribution of the form (1)–(3). More than 99% of the volume under the 3D distribution (2) lies inside an effective domain given by:

$$R_N = \{(x, y, z) : |x - x_c| \leq 3\sigma_x, |y - y_c| \leq 3\sigma_y, |z - z_c| \leq 3\sigma_z\} \quad (7)$$

$$\mathbf{p} = [\mathbf{A}^T \quad \mathbf{r}_c^T \quad \boldsymbol{\sigma}^T]^T \quad (8)$$

We aim in this work to estimate the gradient  $\partial E(k\Delta t)/\partial p_i$ ,  $\forall i$  and  $\forall k$  using only one extra simulation. Here,  $\mathbf{p}$  is the vector of parameters of discontinuities with Gaussian material properties and is given by (8), where  $\mathbf{A}$  is the vector of the amplitudes of the Gaussian distributions,  $\mathbf{r}_c$  is the vector of the centers of the different discontinuities, and  $\boldsymbol{\sigma}$  is the vector of the standard deviations.

Figure 2 shows the effect of a small perturbation of different parameters on the original effective domain for the 2D case. Assuming that  $\sigma_x \neq \sigma_z$ , the effective domain is a rectangle centered at  $(x_c, z_c)$  with length  $6\sigma_x$  and width  $6\sigma_z$  as shown in the shaded region in Fig. 2(a). Assuming a perturbation in  $x_c$  of  $\Delta x_c$ , the new effective area is shifted to the right by  $\Delta x_c$  as shown in the dotted region. Because of the spatial dependence of the Gaussian function, the left gray column is also affected by this perturbation. Fig. 2(b) shows the new effective area in the case of a small perturbation in  $\sigma_x$  by a small change of  $\Delta\sigma_x = \Delta L/3$ . In this case, the length of the effective area is increased by  $6\Delta\sigma_x = 2\Delta L$  equally from both sides. The center of the Gaussian distribution does not change in this case.

In Fig. 2(c), a small change with  $\Delta\theta$  in the distribution orientation results in a rotation of the original area. In the case of a polar Gaussian distribution  $\sigma_x = \sigma_z = \sigma_r$ , the effective area is taken as a circle of radius  $3\sigma_r$  centered at  $(x_c, z_c)$ . A small perturbation of  $\Delta\sigma_r$  increases the radius of the effective area by  $3\Delta\sigma_r$  as shown in Fig. 2(d). As evident from Fig. 2, the perturbed area is different for

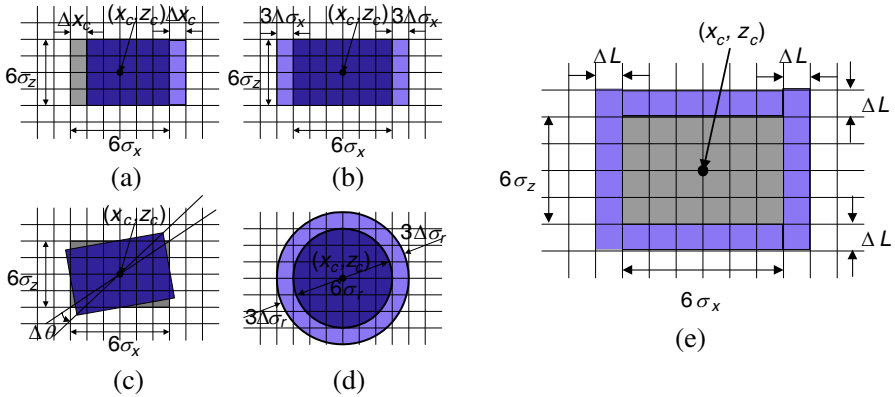


**Figure 2.** The original discontinuity and its new affected areas for different change of parameters such as (a)  $\Delta x_c = \Delta L$ , (b)  $\Delta \sigma_x = \Delta L/3$ , (c) small  $\Delta \theta$ , (d)  $\Delta \sigma_r = \Delta L/3$  in case of polar Gaussian distributions, and (e) the effective area of interest in the case of rectangular Gaussian distribution.

different parameter perturbations. All these affected areas, however, are contained within a domain which is larger than  $R_N$  from each side by  $\Delta L$  as shown in Fig. 2(e). Thus by storing the vectors  $\lambda_{j,k,\tau}$  and  $\eta_{j,k,i}$  in this area, all sensitivities can be calculated. Also, it is emphasized that only one adjoint response  $\lambda_{j,k,\tau}$  is required to estimate the sensitivities with respect to all parameters.

We utilize analytical sensitivities of the nodal scattering matrices ( $\partial \mathbf{S}_j / \partial p_i$ ) instead of ( $\Delta \mathbf{S}_j / \Delta p_i$ ) to improve the accuracy compared to previous techniques. These analytical sensitivities are available if  $p_i$  is a parameter of the Gaussian distribution of either the relative permittivity or the conductivity. The chain rule is applied where the local scattering matrices are differentiated relative to the local permittivity and this permittivity is differentiated relative to the different distribution parameters.

The previous discussion dealt with the case where there is only one discontinuity with Gaussian material distribution. Also, the field sensitivity at only one probe was considered. This approach can be extended to the case of multiple discontinuity and multiple observation probes. We assume that a given structure has  $n$  observation points, and  $m$  different discontinuities  $W_q$ ,  $q = 1, 2, \dots, m$ . These discontinuities are in different positions and each has a different Gaussian material distribution with  $r$  parameters. The derivative  $(\partial E_l(t) / \partial p_{qv})$  is the sensitivity of the probed field component  $E$  at the  $l$ th observation

point with respect to the  $v$ th parameter of the  $q$ th obstacle. We thus have  $n \times m \times r$  sensitivities. The number of extra simulations required to estimate these sensitivities using finite difference approaches would be very large. Using our algorithm, we are able to obtain all these sensitivities by modifying the forward simulation. The sensitivity formula will be:

$$\frac{\partial E_l(\tau)}{\partial p_{qv}} \approx -\Delta t \sum_j \sum_k \left( \boldsymbol{\lambda}_{j,k,\tau}^{l,q} \right)^T \boldsymbol{\eta}_{j,k,v}^{l,q} \quad (9)$$

where  $\boldsymbol{\lambda}_{j,k,\tau}^{l,q}$  is the adjoint variable calculated when the adjoint excitation is applied at the  $l$ th observation point and saved in the  $q$ th obstacle as shown in Fig. 2(e). All the vectors  $\boldsymbol{\eta}_{j,k,v}^{l,q}$  are obtained using the original simulation. A total of  $n$  adjoint simulations are required to obtain all the sensitivities. Note that both the original and adjoint simulations run in parallel. This feature allows for a possible acceleration using parallel processing.

### 3.2. Algorithm

The algorithm of this method can be summarized in the following steps.

- *Input data*: Define the structure, the number of discontinuities, observation probes, and excitations.
- *Distribution functions*: Define the parameters of the Gaussian distribution of each material property for all discontinuities.
- *Excitation function*: Define the excitation sources of the original problem. The Gaussian modulated sinusoid function is the excitation function utilized in this paper and is defined by:

$$f(t) = A \sin(2\pi f_c (t - \bar{t})) \exp\left(-\frac{(t - \bar{t})^2}{2\sigma_t^2}\right) \quad (10)$$

- *Forward Simulation*: Carry out the original simulation (4) with the excitation (10). Determine the vector  $\boldsymbol{\eta}_{j,k,v}^{l,q}$  using Equation (5).
- *Adjoint Simulations*: Carry out the adjoint simulations (5) to obtain  $\boldsymbol{\lambda}_{j,k,\tau}^{l,q}$ .
- *Sensitivity Estimation*: Apply Equation (9) using the available forward and adjoint vectors to estimate all the sensitivities  $(\partial E_l(\tau)/\partial p_{qv}), \forall \tau$ .

#### 4. SENSITIVITY ANALYSIS RESULTS

In this section, we test our approach through 2D and 3D examples. For the 2D case, we consider the structure shown in Fig. 3(a). It shows a rectangular dielectric discontinuity inside a parallel plate waveguide. This domain is discretized into cells of dimensions  $\Delta x = \Delta z = \Delta L = 0.5$  mm. The properties of the background medium are given by  $(\epsilon_{r,m}, \sigma_m) = (3.0, 0.5 \text{ S/m})$ . The observation point is  $r = [7.0 \text{ mm } 30.0 \text{ mm}]^T$ . The number of time steps utilized for all 2D cases is  $k_{\max} = 5000$ . The excitation source is a Gaussian modulated sinusoidal signal with center frequency 3.0 GHz and a bandwidth of 1.0 GHz. The excitation has a uniform spatial distribution along the first column of cells along the  $z$  coordinate. Due to space limitation, we show only part of the sensitivity information obtained using our algorithm. Our AVM sensitivity estimates are compared with those obtained using the central finite difference (CD) approximation.

##### 4.1. $\epsilon_r$ and $\sigma$ with Different Gaussian Distribution

We consider in the first case where  $\epsilon_r$  and  $\sigma$  have different Gaussian distribution parameters. These parameters are given by  $x_{c1} = x_{c2} = 7.0$  mm,  $z_{c1} = z_{c2} = 15.0$  mm,  $\sigma_{x1} = \Delta L = 0.5$  mm,  $\sigma_{z1} = (2/3)$  mm,  $\sigma_{x2} = (5/6)$  mm,  $\sigma_{z2} = 0.5$  mm,  $\epsilon_{r,\max} = 5.0$ ,  $\theta_1 = \pi/4$ ,  $\sigma_{\max} = 0.5 \text{ S/m}$ , and  $\theta_2 = \pi/6$ . The sensitivity analysis of any field component can thus be estimated with respect to all 12 parameters. The sensitivity of the electric field with respect to the maximum peaks  $\{\epsilon_{r,\max}, \sigma_{\max}\}$ ,

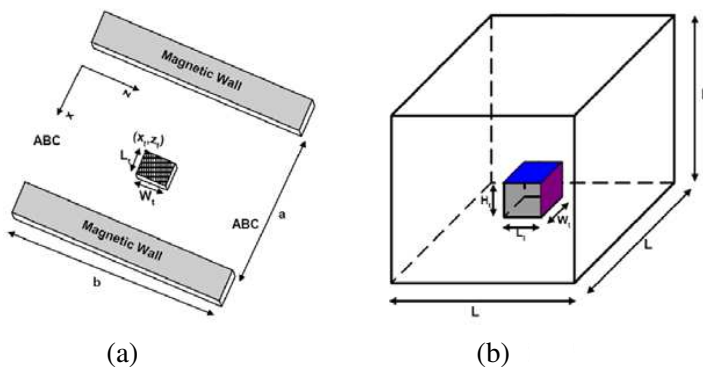


**Figure 3.** The structure of: (a) a 2D dielectric discontinuity example with  $a = 14.0$  mm and  $b = 30.0$  mm, and (b) the 3D dielectric discontinuity example with  $L = 20.0$  mm.

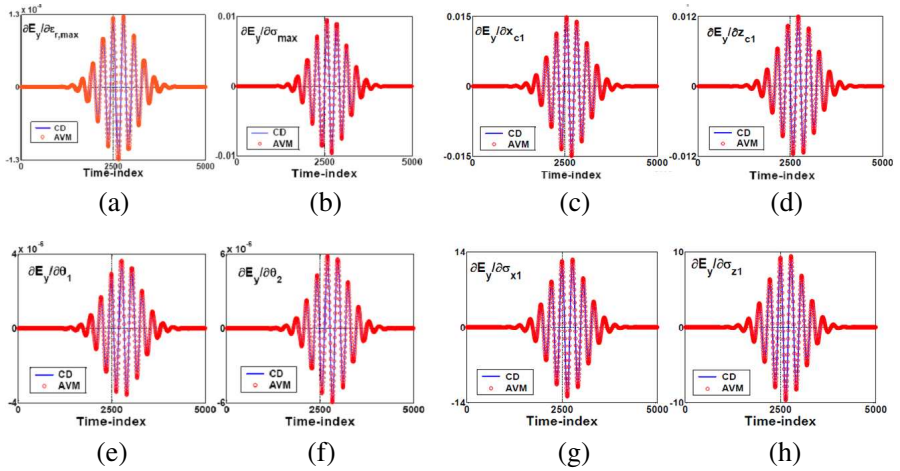


**Figure 4.** The sensitivities of  $\mathbf{E}_y$  with respect to  $\varepsilon_{r,\max}$ ,  $\sigma_{\max}$ ,  $x_{c1}$ ,  $z_{c1}$ ,  $\theta_1$ ,  $\theta_2$ ,  $\sigma_{x1}$ , and  $\sigma_{z1}$  in the case of 2D structure where  $\varepsilon_r$  and  $\sigma$  have different Gaussian distributions.

angles  $\{\theta_1, \theta_2\}$ , center positions  $\{x_{c1}, z_{c1}\}$ , and the standard deviations  $\{\sigma_{x1}, \sigma_{z1}\}$  using both our AVM approach and using the CD techniques are shown in Fig. 4. The CD approach requires 24 extra TLM simulations.

#### 4.2. Polar Gaussian with Multiple Excitation Points

In this example, we consider the case where the standard deviations are the same for both the  $x$  and  $z$  coordinates. We further assume that  $\varepsilon_r$  and  $\sigma$  have the same spatial parameters  $xc = 7.0$  mm,  $zc = 15.0$  mm, and  $\sigma_r = 0.5$  mm. The amplitudes of the Gaussian distributions are given by  $\varepsilon_{r,\max} = 5.0$  and  $\sigma_{\max} = 0.5$  S/m. Two different excitations are applied in this case. The first excitation is a Gaussian modulated point source with a center frequency of 3.0 GHz and a bandwidth of 1.0 GHz. The source is located at the point (0.5, 2.5) mm. The second excitation is also a Gaussian modulated sinusoid with a center frequency of 6.0 GHz and a bandwidth of 2.0 GHz. It is located at the point (0.5, 4.5) mm. The sensitivities of the temporal electric field with respect to all the parameters of the Gaussian distribution of the discontinuity are shown in Fig. 5. Our approach requires only one extra TLM simulation while the CD approach requires 12 additional TLM simulations.

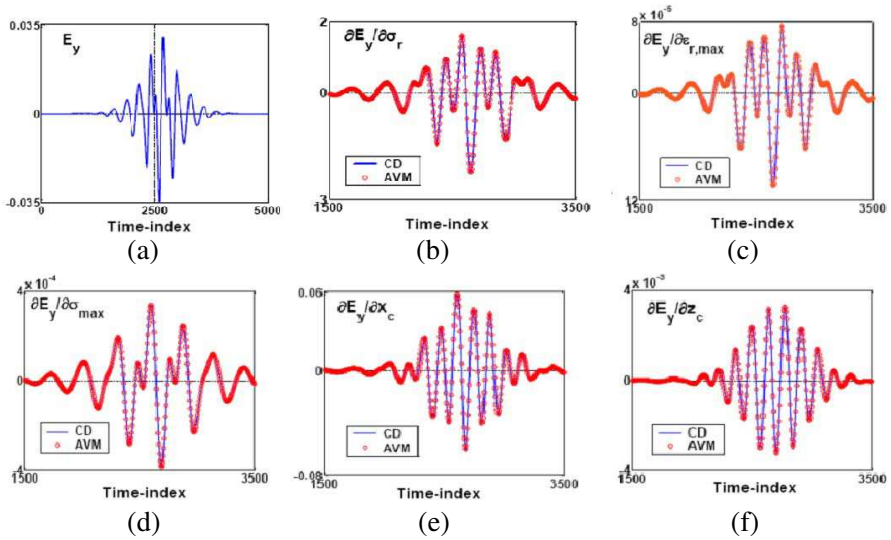


**Figure 5.** The electric field  $E_y$  and its sensitivity with respect to  $\sigma_r$ ,  $\epsilon_{r,\max}$ ,  $\sigma_{\max}$ ,  $x_c$ , and  $z_c$  for the 2D case with multiple excitations.

### 4.3. A 3D Example

We also consider the 3D structure shown in Fig. 3(b). This structure represents a discontinuity with a cubic shape bounded by zero reflection coefficient boundaries. We have only a single obstacle where  $\epsilon_r$  and  $\sigma$  have the same 3D polar Gaussian distribution as in the previous example. The cell size is given by  $\Delta x = \Delta y = \Delta z = 1.0$  mm. A total of  $k_{\max} = 3000$  time steps are utilized. There is a single excitation point with a center frequency of 3.0 GHz and a bandwidth of 1.0 GHz. The excitation point is located at (1.0, 14.0, 20.0) mm. The properties of the host medium are  $\epsilon_{r,m} = 16.0$  and  $\sigma_m = 0.16$  S/m. The observation point is located at (20.0, 10.0, 10.0) mm. We assume that  $\epsilon_r$  and  $\sigma$  have same 3D Gaussian distribution with parameters  $(x_c, y_c, z_c) = (10.0, 10.0, 10.0)$  mm,  $\sigma_{\max} = 1.08$ ,  $\epsilon_{r,\max} = 41.0$ , and  $\sigma_x = \sigma_y = \sigma_z = 1.0$  mm. Fig. 6 illustrates the sensitivities of the electric field  $E_x$  at the observation point with respect to the eight parameters  $\epsilon_{r,\max}$ ,  $\sigma_{\max}$ ,  $x_c$ ,  $y_c$ ,  $z_c$ ,  $\sigma_x$ ,  $\sigma_y$ , and  $\sigma_z$ . Our technique requires only one adjoint simulation while the CD approach requires 16 extra simulations.

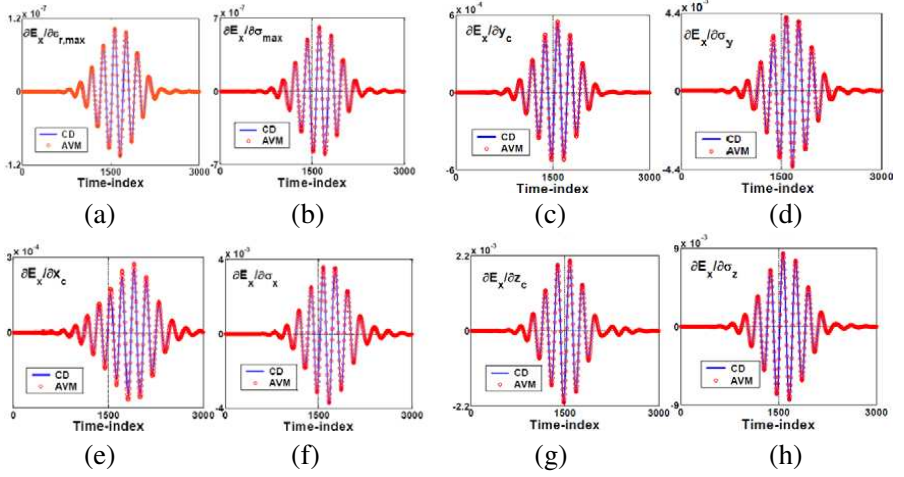


**Figure 6.** The sensitivities of  $E_x$  with respect to  $\varepsilon_{r,\max}$ ,  $\sigma_{\max}$ ,  $y_c$ ,  $\sigma_y$ ,  $x_c$ ,  $\sigma_x$ ,  $z_c$ , and  $\sigma_z$  for the 3D example.

## 5. OPTIMIZATION RESULTS

We utilize our estimated AVM sensitivities in the solution of inverse problems related to microwave imaging. The objective of these inverse problems is to determine the shape, location, and all electromagnetic properties of an unknown scatterer. Many optimization techniques are used for the solution of inverse problems [22–25].

We assume that the scatterer has material properties exhibiting Gaussian distribution. This assumption reduces the number of unknowns of a specific material property to six and seven for the 2D and 3D cases, respectively. Our optimization problem is to find the unknown optimal vector  $\mathbf{p}^*$  whose components are a subset of the Gaussian parameters  $\{\varepsilon_{r,\max}, \sigma_{\max}, x_c, y_c, z_c, \sigma_x, \sigma_y, \sigma_z\}$  that minimizes the objective function:

$$\mathbf{p}^* = \min_{\mathbf{p}} \|\mathbf{F}(\mathbf{p}, t) - \mathbf{F}_{target}(t)\|, \forall t \in [0, t_{\max}] \quad (11)$$

where  $\mathbf{F}(\mathbf{p}, t)$  is the simulator field and  $\mathbf{F}_{target}$  is the target field. The matlab [28] function `fminimax` is utilized in the solution of this problem. Fig. 7 illustrates the geometry of the problem. There is single Gaussian modulated sinusoidal excitation source at (35.0, 1.0) mm with parameters  $f_c = 3.0$  GHz and  $BW = 1.0$  GHz. The square area is a local host with corners at (22.0, 22.0) mm to (44.0, 44.0) mm and with uniform properties  $\varepsilon_{r2} = 40.0$ ,  $\sigma_2 = 3.5$  S/m. The observation point is located at (35.0, 70.0) mm. The background medium has the material

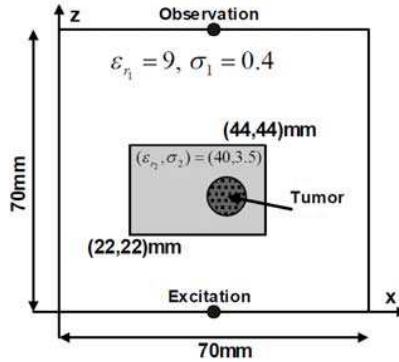


**Figure 7.** The 2D optimization problem.

properties  $\epsilon_{r1} = 9.0$  and  $\sigma_1 = 0.4$  S/m. We assume that  $\epsilon_r$  and  $\sigma$  of the tumor have polar Gaussian distribution. The effective area of the tumor is approximated by a circle of radius  $r = 6\sigma_r$ . We consider the following different optimization problems:

**5.1.**  $\mathbf{p} = [\epsilon_{r,\max} \ \sigma_{\max}]^T$

Here, we fix  $x_c$ ,  $z_c$ , and  $r$ . We optimize only for the amplitudes of the Gaussian distribution of the relative permittivity and conductivity. For this example, we have  $\Delta L = 1.0$  mm and  $k_{\max} = 3000$ . The initial value of the optimization vector  $\mathbf{p}_0 = [40.0 \ 3.5 \text{ S/m}]^T$ . These are the same values as those of the background medium. Table 1 describes two different cases:

- Case 1:  $x_c = z_c = 30$  mm, and  $r = 6.0$  mm.
- Case 2:  $x_c = 40.0$  mm,  $z_c = 30.0$  mm, and  $r = 9.0$  mm.

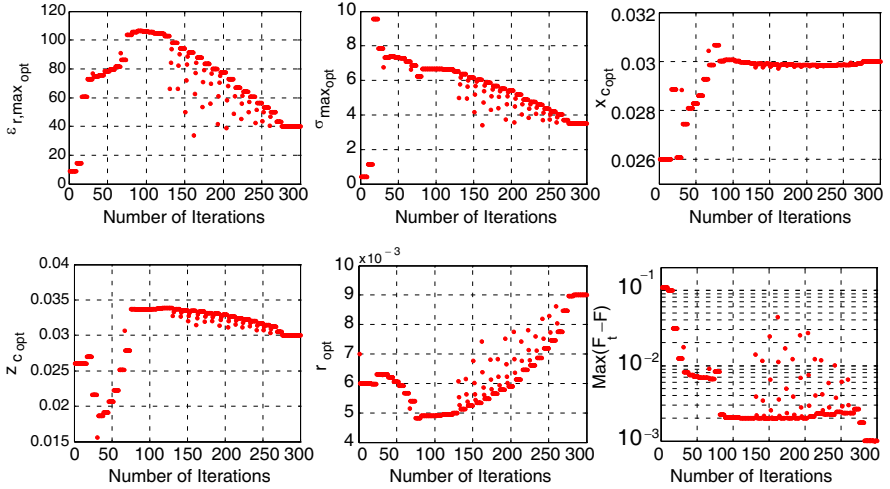
For both cases, using our AVM sensitivities, we are able to successfully recover the amplitudes of the Gaussian distribution.

**5.2.**  $\mathbf{p} = [\epsilon_{r,\max} \ \sigma_{\max} \ x_c \ z_c \ r]^T$  with Noisy Data

To verify the robustness of our approach, we assume that the measured field is contaminated with a Gaussian additive noise. Assume for simplicity that the local host medium is the same as background medium ( $\epsilon_{r2} = 9.0$ ,  $\sigma_2 = 0.4$  S/m). The target material properties are given by  $\mathbf{p}_{\text{target}} = [40.0 \ 3.5 \text{ S/m} \ 30.0 \text{ mm} \ 30.0 \text{ mm} \ 9.0 \text{ mm}]^T$ . Here, we use  $\Delta L = 1.0$  mm,  $k_{\max} = 1500$ , and initial values  $p_o = [9.0 \ 0.4 \text{ S/m} \ 26.0 \text{ mm} \ 26.0 \text{ mm} \ 6.0 \text{ mm}]^T$ . Fig. 8 shows the output optimization

**Table 1.** Optimization results for the case  $\mathbf{p} = (\varepsilon_{r,\max}, \sigma_{\max})$ .

Target values		Case 1		Case 2	
$\varepsilon_{r,\max t}$	$\sigma_{\max -t}$	$\varepsilon_{r,\max f}$	$\sigma_{\max -f}$	$\varepsilon_{r,\max f}$	$\sigma_{\max -f}$
42	3.7	41.999	3.6999	41.999	3.6999
42	6	42.000	6.0000	42.000	6.0000
45	4	44.999	4.0000	45.000	4.0000
45	5	44.999	4.9999	44.999	4.9999
48	4.3	48.000	4.3000	48	4.2999
50	3.7	49.999	3.6999	50.000	3.6999
50	4	50.000	3.9999	50.000	4.0000
50	4.3	50.000	4.3000	50.000	4.3000
55	4	55.000	4.0000	55.000	4.0000
60	6	60.000	6.0000	60.000	6.0000

**Figure 8.** The optimal parameters  $[\varepsilon_{r,\max} x_c z_c r]^T$  and the maximum error versus number of iterations in the case of additive Gaussian noise of 1.0 m V/m.

parameters and the maximum error versus number of iterations in the case of a Gaussian noise with amplitude 0.001 V/m. The final optimal vector is  $\mathbf{p}_{opt} = [39.999 \ 3.4999 \text{ S/m} \ 30 \text{ mm} \ 30 \text{ mm} \ 9.0 \text{ mm}]^T$ . The correct Gaussian distribution is successfully recovered using our adjoint variable sensitivities.

### 5.3. $\mathbf{p} = [\varepsilon_{r,\max} \sigma_{\max} x_c z_c r]^T$

For this case, we assume that the discontinuity has a polar distribution and all of its parameters are unknown. We utilize the step size  $\Delta L = 1.0$  mm and  $k_{\max} = 1500$ . The initial value of the optimization vector is  $\mathbf{p}_0 = [42.0 \text{ S/m } 26.0 \text{ mm } 26.0 \text{ mm } 6.0 \text{ mm}]^T$ . Using actual material properties of  $\mathbf{p}_{target} = [45.0 \text{ S/m } 30.0 \text{ mm } 30.0 \text{ mm } 9.0 \text{ mm}]^T$ , the output result of the optimization algorithm is  $\mathbf{p}^* = [45.0 \text{ S/m } 29.9 \text{ mm } 30.0 \text{ mm } 8.99 \text{ mm}]^T$ . Also, when  $\mathbf{p}_{target} = [50.0 \text{ S/m } 30.0 \text{ mm } 35.0 \text{ mm } 12.0 \text{ mm}]^T$ , the final result was  $\mathbf{p}^* = [50.0 \text{ S/m } 30.0 \text{ mm } 34.99 \text{ mm } 11.99 \text{ mm}]^T$ . Both results show that the optimizer successfully recovered the material properties using our adjoint sensitivities.

### 5.4. $\mathbf{p} = [\varepsilon_{r,\max} \sigma_{\max} x_c z_c r]^T$ “no tumor”

In this case, we test the optimization technique against the case of “false detection”. The supplied values of the field are those of the case where there is no discontinuity. We use  $\Delta L = 1.0$  mm and  $k_{\max} = 1500$ . The initial values of the optimization vector  $\mathbf{p}$  are chosen as in the previous case. The optimal set of optimization parameters is  $\mathbf{p}^* = [40.0 \text{ S/m } 26.06 \text{ mm } 26.06 \text{ mm } 6.0 \text{ mm}]^T$ . The recovered amplitudes of the discontinuity are identical to those of the surrounding local host. This simply means that there is no discontinuity. The last three values are meaningless because a discontinuity with the same material properties as the surrounding medium can be placed anywhere.

### 5.5. $p = [\varepsilon_{r,\max} \sigma_{\max} x_c z_c r]^T$ with No Local Host

The properties of the local host medium are identical to those of the background medium ( $\varepsilon_{r2} = 9.0$ ,  $\sigma_2 = 0.4$  S/m). The target material properties are given by  $\mathbf{p}_{target} = [30.0 \text{ S/m } 32.0 \text{ mm } 32.0 \text{ mm } 9.0 \text{ mm}]^T$ . Using  $\Delta L = 1.0$  mm,  $k_{\max} = 1500$ , and initial values  $\mathbf{p}_0 = [9.0 \text{ S/m } 25.0 \text{ mm } 25.0 \text{ mm } 6.0 \text{ mm}]^T$ , the vector of optimal parameters is  $\mathbf{p}_{opt} = [29.999 \text{ S/m } 31.99 \text{ mm } 31.99 \text{ mm } 9.0 \text{ mm}]^T$ . The properties of the discontinuity are thus successfully recovered using our adjoint variable sensitivities.

### 5.6. $\mathbf{p} = [\varepsilon_{r,\max} \sigma_{\max}]^T$ for the 3D Example

We also consider recovering the properties of the 3D discontinuity shown in Fig. 4(b). The problem has the following parameters  $L = 20$  mm,  $\Delta L = 0.1$  mm,  $k_{\max} = 2000$ ,  $\varepsilon_{r,m} = 40.0$ , and  $\sigma_m = 0.4$  S/m.

The excitation point source is at (1, 14, 20) mm, and the observation point at (20, 10, 20) mm. The optimization problem utilizes the initial parameter values  $\mathbf{p}_0 = [40.0 \ 0.4 \text{ S/m}]^T$ . The target vector of material properties is  $\mathbf{p}_{target} = [50.0 \ 1.0 \text{ S/m}]^T$ . The optimal values are found to be  $[49.999 \ 0.999 \text{ S/m}]^T$ . Fig. 9 shows the maximum error and the change in parameter values as functions of the optimization iterations.

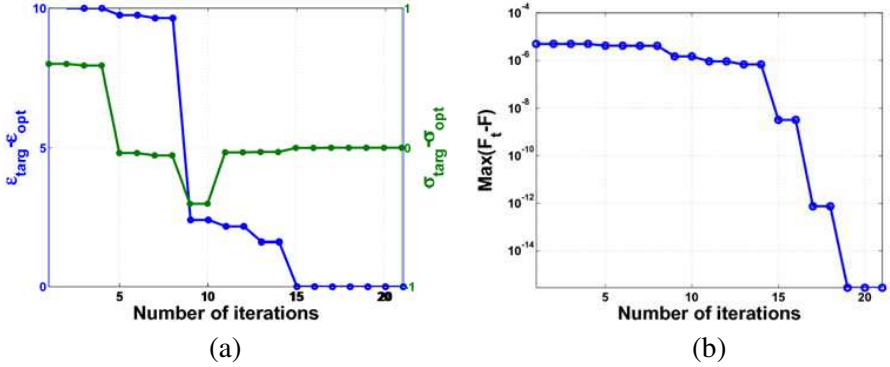


**Figure 9.** (a) The error in calculating  $\varepsilon$ , and (b) the maximum error versus number of iterations.

**Table 2.** Optimization result for the 3D case  $\mathbf{p} = (x_c, y_c, z_c)$ .

Iteration	$x_c$	$y_c$	$z_c$
1	9.0	9.0	9.0
2	9.0	9.0	9.0
3	10.928	9.538	10.129
4	10.928	9.538	10.129
5	9.842	9.734	9.799
6	9.842	9.734	9.799
7	9.762	9.870	9.746
8	9.762	9.870	9.746
9	10.001	9.990	10.003
10	10.001	9.990	10.003
11	9.999	9.999	9.999
12	9.999	9.999	9.999
13	10.000	10.000	10.000

### 5.7. $\mathbf{p} = [x_c \ y_c \ z_c]^T$ for the 3D Example

In this example, we solve for the center of the Gaussian distribution. We use the values  $\varepsilon_{r,\max} = 57.0$ ,  $\sigma_{\max} = 0.5 \text{ S/m}$ ,  $r = 6.0 \text{ mm}$ ,  $\varepsilon_{r,m} = 40.0$ ,  $\sigma_m = 0.4 \text{ S/m}$ ,  $L = 30 \text{ mm}$ ,  $k_{\max} = 1000$ , and  $\Delta L = 1.0 \text{ mm}$ . The initial values of the optimization problem are  $\mathbf{p}_0 = [9.0 \text{ mm} \ 9.0 \text{ mm} \ 9.0 \text{ mm}]^T$ . The target values of  $\mathbf{p}_{\text{target}} = [10.0 \text{ mm} \ 10.0 \text{ mm} \ 10.0 \text{ mm}]^T$ . Table 2 shows the output optimization vector at different iterations.

## 6. CONCLUSION

We present a novel adjoint variable method approach that obtains the sensitivities of a transient time domain response with respect to the dielectric discontinuities with Gaussian material properties. We show that by using only one adjoint simulation, the sensitivities with respect to all parameters of the Gaussian distribution are obtained. We consider different cases for both 2D and 3D TLM simulations. Excellent sensitivity estimates are obtained for a number of examples. We exploit our adjoint sensitivities to recover the unknown parameters of the dielectric discontinuities through given transient field response. Same procedure can be applied to inverse problems using electromagnetic imaging for 2D and 3D structures having any numbers of obstacles or discontinuities with different material distributions.

## REFERENCES

1. Feehery, W. F., J. E. Tolsma, and P. I. Barton, "Efficiently sensitivity analysis of large-scale differential-algebraic systems," *Applied Numerical Mathematics*, Vol. 25, 41–54, 1997.
2. Cao, Y., S. Li, L. Petzold, and R. Serban, "Adjoint sensitivity analysis for differential-algebraic equations: The adjoint DAE system and its numerical solution," *SIAM J. Sci. Comput.*, Vol. 24, 1076–1089, 2003.
3. Li, S. and L. Petzold, "Adjoint sensitivity analysis for time-dependent partial differential equations with adaptive mesh refinement," *Journal of Computational Physics*, Vol. 198, 310–325, 2004.
4. Ding, J.-Y., Z.-K. Pan, and L.-Q. Chen, "Second order adjoint sensitivity analysis of multibody systems described by differential-algebraic equations," *Multibody Syst. Dyn.*, Vol. 18, 599–617, 2007.
5. Errico, R. M., "What is an adjoint model?" *Bulletin of the American Meteorological Society*, Vol. 78, 2577–2591, 1997.

6. Vallese, L. M., "Incremental versus adjoint models for network sensitivity analysis," *IEEE Trans. Circuits & Systems*, Vol. 21, No. 1, 46–49, 1974.
7. Lee, H., "Adjoint variable method for structural design sensitivity analysis of a distinct eigenvalue problem," *KSME International Journal*, Vol. 13, No. 6, 470–476, 1999.
8. Chung, Y.-S., J. Ryu, C. Cheon, I. H. Park, and S.-Y. Hahn, "Optimal design method for microwave devices using time domain method and design sensitivity analysis — Part I: FETD case," *IEEE Trans. on Magnetics*, Vol. 37, No. 5, 3289–3293, Sep. 2001.
9. Webb, J. P., "Design sensitivity of frequency response in 3-D finite-element analysis of microwave devices," *IEEE Trans. Magnetics*, Vol. 38, 1109–1112, 2002.
10. Basl, P. A. W., M. H. Bakr, and N. K. Nikolova, "The theory of self-adjoint S-parameter sensitivities for lossless nonhomogeneous TLM problems," *IET Microw. Antennas Propagation*, Vol. 2, No. 3, 211–220, 2008.
11. Drogoudis, D. G., G. A. Kyriacou, and J. N. Sahalos, "Microwave tomography employing an adjoint network based sensitivity matrix," *Progress In Electromagnetics Research*, Vol. 94, 213–242, 2009.
12. Chung, Y. S., C. Cheon, I. H. Park, and S. Y. Hahn, "Optimal design method for microwave device using time domain method and design sensitivity analysis — Part II: FDTD case," *IEEE Trans. Magn.*, Vol. 37, 3255–3259, Sep. 2001.
13. Bakr, M. H. and N. K. Nikolova, "An adjoint method for time domain transmission-line-modeling with fixed structured grids," *IEEE Trans. Microwave Theory Tech.*, Vol. 52, 554–559, Feb. 2004.
14. Bakr, M. H. and N. K. Nikolova, "An adjoint variable method for time domain TLM with wide-band John matrix boundaries," *IEEE Trans. Microwave Theory Tech.*, Vol. 52, 678–685, 2004.
15. Nikolova, N. K., H. W. Tam, and M. H. Bakr, "Sensitivity analysis with the FDTD method on structured grids," *IEEE Trans. Microwave Theory Tech.*, Vol. 52, No. 4, 1207–1216, Apr. 2004.
16. Nikolova, N. K., Y. Li, and M. H. Bakr, "Sensitivity analysis of scattering parameters with electromagnetic time-domain simulators," *IEEE Trans. Microwave Theory Tech.*, Vol. 54, No. 4, 1598–1610, Apr. 2006.
17. Song, Y., Y. Li, N. K. Nikolova, and M. H. Bakr, "Self-adjoint sensitivity analysis of lossy dielectric structures with

- electromagnetic time domain simulators,” *Int. J. Numer. Model.*, Vol. 21, 117–132, Oct. 2007.
18. Bakr, M. H., P. Zhao, and N. K. Nikolova, “Adjoint first order sensitivities of time domain responses and their applications in solution of inverse problems,” *IEEE Trans. Antennas Propagat.*, Jul. 2009.
  19. Ozyurt, B. D. and P. I. Barton, “Large-scale dynamic optimization using the directional second-order adjoint method,” *Ind. Eng. Chem. Res.*, Vol. 44, 1804–1811, 2005.
  20. Georgieva, N. K., S. Glavic, M. H. Bakr, and J. W. Bandler, “Feasible adjoint sensitivity technique for EM design optimization,” *IEEE Trans. Microwave Theory Tech.*, Vol. 50, 2751–2758, Dec. 2002.
  21. Nikolova, N. K., R. Safian, E. A. Soliman, and M. H. Bakr, “Accelerated gradient based optimization using adjoint sensitivities,” *IEEE Trans. Antennas Propagat.*, Vol. 52, 2147–2157, Aug. 2004.
  22. Goharian, M., M. Soleimani, and G. R. Moran, “A trust region subproblem for 3D electrical impedance tomography inverse problem using experimental data,” *Progress In Electromagnetics Research*, Vol. 94, 19–32, 2009.
  23. Mojabi, M. and J. LoVetri, “Adapting the normalized cumulative periodogram parameter-choice method to the Tikhonov regularization of 2-D/TM electromagnetic inverse scattering using Born iterative method,” *Progress In Electromagnetics Research*, Vol. 1, 111–138, 2008.
  24. Yu, C., M. Yuan, and Q. H. Liu, “Reconstruction of 3D objects from multi-frequency experimental data with a fast DBIM-BCGS method,” *Inverse Problems*, 25, doi:10.1088/0266-5611/25/2/024007, 2009.
  25. Bindu, G., A. Lonappan, V. Thomas, C. K. Aanandan, K. T. Mathew, and S. J. Abraham, “Active microwave imaging for breast cancer detection,” *Progress In Electromagnetics Research*, Vol. 58, 149–169, 2006.
  26. Johns, P. B. and R. L. Beurle, “Numerical modeling of 2-dimensional scattering problems using a transmission line matrix,” *Proceedings of IEE*, Vol. 118, No. 9, 1203–1208, Sep. 1971.
  27. Christopoulos, C., *The Transmission-line-method TLM*, IEEE Press, 1995.
  28. Matlab, Version 7.0.1, 2004.